



Published in final edited form as:

Nutr Cancer. 2014 ; 66(2): 285–294. doi:10.1080/01635581.2014.868912.

Benzyl Isothiocyanate Inhibits HNSCC Cell Migration and Invasion, and Sensitizes HNSCC Cells to Cisplatin

M. Allison Wolf^{a,b} and Pier Paolo Claudio^{a,b,c,*}

M. Allison Wolf: teter6@marshall.edu; Pier Paolo Claudio: claudiop@marshall.edu

^aMcKown Translational Genomic Research Institute, Joan C. Edwards School of Medicine, Marshall University, Huntington, WV 25701, USA

^bDepartment of Biochemistry and Microbiology, Joan C. Edwards School of Medicine, Marshall University, Huntington, WV 25755, USA

^cDepartment of Surgery, Joan C. Edwards School of Medicine, Marshall University, Huntington, WV 25701, USA

Abstract

Metastasis and chemoresistance represent two detrimental events that greatly hinder the outcome for those suffering with head and neck squamous cell carcinoma (HNSCC). Herein, we investigated benzyl isothiocyanate's (BITC) ability to inhibit HNSCC migration and invasion and enhance chemotherapy. Our data suggests that treatment with BITC: 1) induced significant reductions in the viability of multiple HNSCC cell lines tested (HN12, HN8, and HN30) after 24 and 48 hours, 2) decreased migration and invasion of the HN12 cells in a dose dependent manner, 3) inhibited expression and altered localization of the epithelial-mesenchymal transition (EMT) marker, vimentin. We also observed that a pretreatment of BITC followed by cisplatin treatment 1) induced a greater decrease in HN12, HN30, and HN8 cell viability and total cell count than either treatment alone, and 2) significantly increased apoptosis when compared to either treatment alone. Taken together these data suggest that BITC has the capacity to inhibit processes involved in metastasis and enhance the effectiveness of chemotherapy. Consequently, the results indicate that further investigation, including *in vivo* studies, are warranted.

Keywords

Head and Neck Squamous Cell Carcinoma; isothiocyanate; BITC; migration; invasion; EMT; vimentin; Benzyl isothiocyanate; cisplatin; chemosensitivity; HNSCC

INTRODUCTION

Head and neck squamous cell carcinoma (HNSCC) is the 6th most common form of cancer worldwide, and the 8th leading cause of cancer-related deaths (1). Current treatment for HNSCC often entails a disfiguring and risky surgical operation, combined with chemotherapy and/or radiation therapy (2–4). These treatment options are associated with numerous side effects that dramatically affect a patient's quality of life, and despite the aggressive treatment options the increase in overall survival of HNSCC has not improved in the past three decades (1, 4–7). The low survival rate is due, in part, to both loco-regional and distant metastasis, which occurs in 40–60 percent of HNSCC patients (4, 7, 8).

*Corresponding author: Pier Paolo Claudio, McKown Translational Genomic Research Institute, Joan C. Edwards School of Medicine, Huntington, West Virginia, 25701, Phone: 304-696-3516, claudiop@marshall.edu.

Additionally, the rate of HNSCC metastasis after recurrence is high, and relapse/recurrence is associated with heightened chemoresistance (7).

A common chemotherapeutic drug used for HNSCC is cisplatin, but the side effects associated with effective treatment doses can be severe. Additionally, one of the major obstacles in the therapeutic use of cisplatin is intrinsic or acquired resistance. Therefore, adjuvant therapies that enhance the efficacy of cisplatin and/or decrease the amount of cisplatin needed to achieve tumor response could improve patient outcome.

The acquisition of chemoresistance and the initiation of metastasis are a complex multistep processes. The use of natural products, such as isothiocyanates (ITCs), which are known to target many cellular pathways linked to both of these processes, provides a unique therapy option for HNSCC. ITCs are phytochemicals produced by several plant species, particularly cruciferous vegetables (9, 10). ITCs are a product of glucosinolate hydrolysis, which is initiated by an enzyme called myrosinase (11). This enzyme is found spatially separated from glucosinolates in cruciferous vegetables and in our own human enteric microflora (11). The reactive group of ITCs, R-N=C=S, plays a significant role in ITCs involvement in numerous cellular pathways (12). This functional group is known to target cysteine residues, which are often found in the catalytic site of many enzymes, and thereby can induce a wide range of effects inside a cell (13, 14).

Benzyl isothiocyanate (BITC) is an ITC of particular interest in cancer therapy because of its ability to inhibit cell growth and induce apoptosis in several types of cancer cell lines, including HNSCC (11, 15, 16). In addition to inhibiting cell growth and inducing apoptosis BITC may play a role in inhibiting angiogenesis, epithelial-mesenchymal transition (EMT), and metastasis (17–19).

The present study builds on recent findings, which indicate that BITC may be able to inhibit metastasis and increase chemosensitivity. The evidence suggests that ITCs may prevent migration and invasion of several types of cancer cells, but the role of BITC in prevention of HNSCC migration and invasion has not been investigated. We elected to focus on BITC over other ITCs because our preliminary screenings suggested that the concentrations needed to elicit a response in HNSCC appear to be lower than other ITCs studied. Through the use of various *in vitro* studies we are reporting for the first time that BITC can inhibit migration and invasion of HNSCC cell lines. The potential use of BITC as an adjuvant treatment to inhibit metastasis, decrease markers associated with EMT, and enhance chemotherapy is a novel treatment approach.

MATERIALS AND METHODS

Materials

Benzyl isothiocyanate (99.5% pure) was purchased from LKT Laboratories, Inc. (St. Paul, MN). Stock solutions of BITC (100mM) were prepared in DMSO and diluted into growth medium such that the final concentration of DMSO did not exceed 0.02% (v/v), a concentration that did not induce toxicity in HN12, HN30, HN8, and HAK cells. Cis-Diammineplatinum (II) dichloride (CDDP) was purchased from Sigma-Aldrich (St. Louis, MO). Stock concentrations of CDDP (1mg/1mL) were prepared in a 0.9% sterile saline solution.

Cell Culture and Reagents

The highly metastatic HNSCC cell line, HN12, and moderately metastatic HNSCC cell line, HN30, were a kind gift from Dr. George Yoo (Karmanos Cancer Center, Wayne State University, OH) (6). The HN8 cell line was a gift from Dr. J. Silvio Gutkind (NIH,

Bethesda, MD) (20). The normal human adult keratinocyte cell line, HAK, was obtained from Zen-Bio, Inc. (Research Triangle Park, NC). Monolayer cultures of HN12, HN30 and HN8 were maintained in DMEM medium (HyClone, Thermo-Scientific) adjusted to contain 10% fetal bovine serum (FBS) (PAA Laboratories GmbH, Pasching, Austria) and supplemented with 1% (vol./vol.) penicillin-streptomycin (P/S) (Corning Cellgro, Manassas, VA). HAK cells were maintained in Adult Keratinocyte Growth Medium (KM-2) (Zen-Bio, Research Triangle Park, NC). Cells were grown in a humidified incubator at 37°C and with 5% CO₂.

MTT Cell Viability Assay

HN12, HN8, and HN30 cells were seeded at an initial density of 5×10^3 cells/well and HAK cells were seeded at an initial density of 15×10^3 cells/well in 96-well tissue culture plates (Corning, Corning, NY) and allowed to settle overnight. The seeding density was selected so that all cell lines had a similar confluence after 24 hours. Cells were subsequently treated with 1.25–10 μM BITC for 1-hour. After 1-hour plates were washed and media was replaced with fresh DMEM. The cell viability was determined after 24- and 48-hours using thiazolyl blue tetrazolium bromide (Sigma-Aldrich, St. Louis, MO). Cells were incubated with dye for 2 hours, and then media was removed and replaced with DMSO. Color development in the plates was read at 590nm using the SpectraMax M2^e plate reader (Molecular Devices, Sunnyvale, CA). The intensity of the color is correlated with the metabolic activity of living cells.

Wound Healing Assay

Cell migration was determined using wound healing assay. HN12 cells were cultured in DMEM (10% FBS, 1% Pen-Strep) in 6-well plates until 90% confluent, and then media was changed to DMEM with 0.05% FBS, 1% P/S overnight to synchronize the cells. A permanent line was drawn horizontally on the bottom of each well, and a plastic pipette tip was used to generate 3 vertical scratches per well. Cell debris was washed away with PBS and initial scratch sizes were determined with an inverted light microscope (Olympus IX51, Center Valley, PA) at 100X magnification. Six measurements were made per well, 1 below and 1 above the horizontal line for each scratch before treatment. Cells were treated with 2.5–5 μM BITC for 1-hour at 37°C. DMSO, at the same concentration as in the BITC treated wells, was used for the vehicle control. After 1-hour plates were washed with PBS and treatment was replaced with DMEM (10% FBS, 1% P/S). Wound healing was analyzed 24 hours after treatment. Images were taken at 100X magnification, as described above, and changes in cell migration were determined by calculating the percent of wound healing. Percent wound healing = $([\text{scratch}_{t=0\text{hr}} - \text{scratch}_{t=24\text{hr}}] / \text{scratch}_{t=0\text{hr}}) * 100$. Experiments were repeated 3 times.

Invasion Assay

The effect of BITC on invasion of HN12 cells was determined using Invasion Chambers with 8 μm pores (BD Biocoat, Franklin Lakes, NJ). Polycarbonate membranes on the bottom of the Boyden chamber inserts were rehydrated following manufacturer's instructions and 0.5mL of HNSCC cell suspension containing 5×10^4 cells was added to each insert. Cells were allowed to attach for 4 hours prior to treatment in complete DMEM media (10% FBS, 1%P/S). After attachment the appropriate wells were treated for 1-hour with BITC (2.5–5 μM) in serum free DMEM. Epidermal growth factor (EGF) was used at (10ng/1mL in serum free DMEM (0.5% BSA, 1% P/S)) was added to the bottom well in all wells, except for the negative control, as a chemoattractant. Media in all inserts was replaced after 1-hour with DMEM (0.5% BSA, 1% P/S). Analysis of cell invasion was performed 24 hours after beginning treatment. Media and cells were removed from the top of the matrigel following manufactures' instructions and cells were fixed with 100% methanol, washed with PBS, and

stained with 0.1% Crystal Violet. Cells counts were performed and images taken using an Olympus IX51 inverted light microscope (Olympus, Center Valley, PA) at 400X magnification. Twenty fields of view were counted for each sample and averaged to determine the mean number of cells/field of view. Experiments were repeated a minimum of 3 times.

Western Blot Analysis

HNSCC cells were treated with BITC for 24 hours. Cell pellets were lysed with RIPA buffer (1% NP-40, 0.1% SDS, 50mM Tris-HCl pH 7.4, 150mM NaCl, 0.5% Sodium Deoxycholate, 1mM EDTA) for analysis. Vimentin antibody (AVIVA, San Diego, CA) was used at a 1:1000 dilution in a 5% milk/TBST buffer. Horseradish peroxidase-conjugated goat anti-rabbit secondary antibody (Rockland, Gilbertsville, PA) was used (1:10,000). The signal was developed with ECL Prime western blotting detection reagent (Amersham, Piscataway, NJ). Densitometry was calculated using α -actin (SantaCruz, Santa Cruz, CA) as a loading control for all Western blots.

Indirect Immunofluorescence

HN12 cells were seeded initially at a density of 4×10^4 in Nunc Lab Tek II immunofluorescence chambers (Fisher Scientifics, Pittsburgh, PA). Cells were allowed to attach overnight before treatment with BITC (5–10 μ M) for 1-hour. Treatment media was then removed and replaced with complete DMEM (10%FBS, 1%P/S). Twenty-four hours after treatment, cells were fixed with 4% paraformaldehyde and permeabilized in PBS containing 1% BSA and 0.1% Triton X-100. Cells were blocked with PBS/1% BSA prior to staining. Vimentin (AVIVA, San Diego, CA) was diluted 1:400 with PBS containing 1% BSA and appropriate wells were incubated with primary antibody in a dark humidified chamber for 1-hour. Cells were then washed and incubated with Alexa Fluor 488 (Invitrogen, Grand Island, NY) secondary antibody (1:200) in humid and dark conditions for 45 minutes. Slides were detached from immunofluorescence chambers and Vectashield mounting media with DAPI (Vector Laboratories, Burlingame, CA) was added to slides before analysis. Images taken using an Olympus IX51 inverted microscope equipped with epifluorescence (Olympus, Center Valley, PA).

MTT Cell Viability/Chemosensitivity Assay

HN12, HN8, and HN30 cells were seeded at an initial density of 5×10^3 cells/well in Corning 96-well tissue culture plates (Corning, NY) and allowed to settle overnight. Cells were then treated with 2.5–10 μ M BITC for 1-hour, 5–10 μ M of CDDP for 24 hours, or a 1-hour pretreatment of 2.5–10 μ M BITC followed by a treatment of 5–10 μ M of CDDP for 24 hours. Media was changed in all wells 24 hours after cisplatin treatment prior to the 48-hour analysis. Cell viability was determined 24 or 48 hours later as described above under MTT Cell Proliferation/Viability Assay methods. Results were performed in technical quadruplets with three biological replicates.

Trypan Blue Dead/Live Assay

HN12, HN8, and HN30 cells were seeded at an initial density of 3×10^5 cells/well in Corning 6-well tissue culture plates (Corning, NY) and allowed to settle overnight. Cells were then treated with 5–10 μ M BITC for 1-hour, or 10 μ M of CDDP for 24 hours, or a 1-hour pretreatment with 5–10 μ M BITC followed by 10 μ M of CDDP for 24 hours. Cell counts were performed 24 and 48 hours after initiating CDDP treatment. Cells were trypsinized and washed in PBS prior to cell count. Cells in each treatment group were mixed 1:1 with a trypan blue solution (0.4% trypan blue in PBS) and counted using a hemacytometer.

Annexin-V/PI Assay

HN12 and HN30 cells were seeded at an initial density of 2×10^6 cells in 10cm Corning tissue culture dish (Corning, NY) and allowed to settle overnight. Cells were treated as described above in the Dead/Live assay methods. Treatment-induced cell death was determined by flow cytometry using an Annexin-V assay kit (eBiosciences, San Diego, CA). 24 and 48 hours after initiating CDDP treatment cells were collected and 1×10^6 cells per group were subjected to a double staining with an Annexin-V-FITC antibody and Propidium Iodide following the manufacturer's instructions.

Statistical Analysis

All experiments were performed at least three times as independent experiments. Statistical analyses were done with a multiple comparison test with appropriate post-hoc test. GraphPad Prism (La Jolla, CA) was used for all statistical analysis. A p -value of <0.05 was considered statistically significant. The combination index of BITC and cisplatin combination was analyzed using the following equation: $CI = (C_{A,x}/IC_{x,A}) + (C_{B,x}/IC_{x,B})$ as described in Zhao et al. (21).

In this equation CI is the combination index; CA, x and CB, x are the concentration of drugs A and B used in a combination that generates x% of the maximal combination effect; IC_x is the drug concentration needed to produce x% of the maximal effect. A CI of less than, equal to, and more than 1 indicates synergy, additivity, and antagonism, respectively.

RESULTS

BITC Decreased the Cell Viability of Three HNSCC Cell Lines

MTT assay results indicate that a 1-hour treatment of $10 \mu\text{M}$ BITC significantly decreased the cell viability ($p < 0.05$) of the HN12, HN8 and HN30 cell lines after 24 and 48 hours (Fig. 1A and B). However, a 1-hour treatment of 2.5 – $5 \mu\text{M}$ BITC did not significantly affect the cell viability of these HNSCC cell lines after 24 hours, and at 48 hours a significant decrease in cell viability was only observed in the HN30 cell line after a $5 \mu\text{M}$ BITC treatment (Fig. 1A and B). Treatment of the normal keratinocyte cell line (HAK) with 2.5 – $10 \mu\text{M}$ BITC did not decrease viability (Fig. 1A and B). Thus BITC has selective toxicity for HNSCC cancer cells. A 1-hour treatment was selected for future experiments because the cell viability of HNSCC cells was not significantly different whether treated with 2.5 – $10 \mu\text{M}$ BITC for 1, 16, or 24 hours (data not shown).

BITC Inhibited Migration and Invasion of HNSCC Cells

A wound-healing assay indicated that BITC inhibits migration of the highly metastatic HN12 cells in a dose dependent manner. After 24 hours, inhibition of cellular migration was seen in the highly metastatic HN12 cell line when using a $2.5 \mu\text{M}$ BITC treatment, however a significant decrease in wound healing required $5 \mu\text{M}$ BITC ($p < 0.05$) (Fig. 2A and B). Similar results were observed when using the HN8 cell line, but the HN30 cell line (data not shown). Although, it should be noted that the HN30 cell line did not undergo “wound-healing” under control conditions.

The ability of BITC to inhibit the migration of HN12 cells prompted us to investigate the effect of BITC on invasion through Matrigel. Figures 3 (panels A and B) depict that 1-hour treatment of BITC significantly inhibited the invasion of HN12 cells ($p < 0.05$). Compared to the vehicle control the number of invading cells per field of view decreased by 52.34% after $2.5 \mu\text{M}$ and 90.96% after a $5 \mu\text{M}$ BITC treatment ($p < 0.05$). Viability assays confirmed that the addition of the chemo-attractant, EGF, to the cells did not change the viability and

proliferation of HNSCC cells after BITC treatment (data not shown). These results substantiate the wound-healing assay data and indicate that BITC targets both migration and invasion of certain HNSCC cell lines.

Vimentin Expression Decreased after BITC Treatment

Vimentin is an intermediate filament protein associated with EMT and HNSCC cell invasion (22, 23). We determined BITC treatment alters vimentin expression or localization. We observed that vimentin expression was inhibited 24 hours after a 1-hour BITC treatment (2.5–10 μ M), in a dose dependent manner (Fig. 4A). The localization of vimentin also appeared altered after BITC treatment. In the vehicle control vimentin was evenly dispersed, and was also observed in cellular projections. However, after BITC treatment these projections disappeared, and vimentin was observed as aggregates inside the cells. Our immunofluorescence results are supported by Western blot analysis showing a significant decrease in vimentin expression was occurred after a 24 hour BITC treatment of 5 and 10 μ M (p 0.05) (Fig. 4B and C). Although the treatment conditions changed for the Western blot analysis, cellular viability of HNSCC cells did not change whether treated with BITC for 1, 16, or 24 hours (data not shown).

Pretreatment with BITC Followed by Cisplatin Decreased HNSCC Cell Viability and Enhanced Cell Death

One of the major obstacles in the therapeutic use of platinum analogues is intrinsic or acquired resistance (24–27). The high cisplatin resistance observed in our HNSCC cell lines prompted us to investigate whether BITC treatment of HNSCC cells enhances their response to CDDP.

A 1-hour pretreatment of BITC enhanced the effect of CDDP after 24 and 48 hours, compared to either BITC or CDDP treatment alone (p 0.05) (Fig. 5A–C). The strongest decrease in cell viability was observed at 48 hours when the HNSCC cells were pretreated with 10 μ M BITC followed by 10 μ M CDDP treatment (Combination index CI= 0.52 to 0.93) (p 0.0001) (Fig. 5A–C). Combination of 10 μ M BITC and 10 μ M cisplatin showed a synergistic effect in HN8 cells at 48 hours (CI= 0.73), but only additive effect at 24 hours (CI= 1.09). A synergistic effect was also observed at 24 and 48 hours in HN30 (24 hours CI= 0.79; 48 hours CI= 0.52) and HN12 cells (24 hours CI= 0.86; 48 hours CI= 0.93) following a combination treatment of 10 μ M BITC and 10 μ M cisplatin (Fig. 5).

The MTT assay assesses changes in cell viability, however the MTT assay does not differentiate between growth inhibition and/or cell death. Therefore, we used a trypan blue dead/live assay and an Annexin-V assay (apoptosis) to determine if BITC pretreatment increased cell death. The trypan blue dead/live assay (Fig. 6A, B, D, E, G, and H) indicated that cell death was significantly enhanced by BITC pretreatment followed by CDDP in all three HNSCC cells (HN8, HN12, and HN30), compared to treatment with either compound alone. However, the most dramatic increase in cell death was observed when HN30 cells were pretreated for 1-hour with 10 μ M BITC followed by a 24-hour 10 μ M CDDP treatment (Fig. 6D, synergistic effect CI= 0.9; p 0.0001). These results were verified by numerical cell counts at the 24 and 48 hour time points of the different treatment groups (Fig. 6C, F, and I). An Annexin-V assay showed a significant increase in early and late apoptosis after a pretreatment of 10 μ M BITC followed by 10 μ M CDDP in both the HN30 and HN12 cell lines after 24 hours (p 0.001) (Fig. 7 A and B). Additionally, the total percent of dead cells (early, late apoptosis, and necrosis) increased significantly when cells were pretreated for 1-hour with 10 μ M BITC followed by a 24-hour 10 μ M CDDP treatment (p 0.0001). Together the results of the MTT assay, dead/live assay, cell counts, and Annexin-V assay show that

pretreatment of HNSCC cells with BITC followed by CDDP significantly increased HNSCC cell death relative to either agent used as a single therapeutic.

DISCUSSION

The treatment for HNSCC often involves a disfiguring surgical operation and either prior or subsequent chemotherapy and/or radiation therapy (1, 28). These combined treatment modalities are often associated with side effects that reduce the patient's quality of life. HNSCC metastasis and chemoresistance are two of the leading reasons for this multimodal treatment approach. The inability to effectively target these events, whether separately or together, leads to a poor prognosis. Consequently, those who suffer from aggressive HNSCC face a debilitating disease, and need improved therapeutic options.

ITCs are natural compounds exhibiting potent anti-tumor effects in both cell culture and animal models (18, 29–31). In humans, ITCs are safe at clinically relevant concentrations and have high oral bioavailability, making them promising adjuvant therapy tools for the treatment of cancer (11, 29, 32). Here, we show that BITC inhibits HNSCC cell migration and invasion, as well as sensitizes HNSCC cells to the chemotherapeutic drug cisplatin at clinically relevant concentrations (19, 30). Additionally, BITC decreased the expression of vimentin, a marker associated with EMT, in the HN12 cell line.

Tumors are not homogenous and may have different aberrant pathways that contribute to maintenance of cancer phenotype. The type of mutations present in different cancer cell could play a significant role on the different pathways and molecular targets of BITC. Since BITC's targets appear to be multifactorial we decided to focus primarily on the end points of cell death, proliferation, migration and invasion. Collectively our results illustrate that the effects of BITC, in regards to migration/invasion and chemoenhancement (greater anti-neoplastic effect than the sum of BITC or CDDP treatment alone) are not cell line specific. Importantly, BITC selectively targeted the viability of HNSCC cells, but not normal keratinocytes (Fig. 1).

Vimentin expression in epithelial cells is a marker for epithelial-mesenchymal transition (EMT). Vimentin's overexpression in HNSCC correlates well with accelerated tumor growth, invasion, and poor prognosis (33). Therefore, vimentin serves as an attractive potential target for HNSCC therapy. Many EMT markers are correlated with poor HNSCC prognosis, but few therapies have been shown to actually regulate the expression of these markers. Additionally, EMT, directly or indirectly links HNSCC metastasis and chemoresistance. Our findings that BITC treatment decreases vimentin expression in HNSCC cells suggest these cells are less likely to undergo EMT following BITC exposure indicating a unique property of this phytochemical that could be exploited for therapy.

Despite significant improvements in treatment modalities, long-term survival rates in patients with advanced-stage HNSCC have not increased significantly in the past 30 years. Radiation and chemotherapy are nonselective and can cause damage to normal tissue. Cisplatin is one example of a non-selective drug commonly used to treat HNSCC. This drug is associated with many detrimental side-effects. Additionally, intrinsic or acquired resistance to platinum analogues is a major obstacle in HNSCC therapy. The results of our MTT assay, dead/live assay, cell counts, and Annexin-V assay support the use of BITC to either counteract cisplatin resistance or enhance its activity (Fig. 5 and Fig. 6). The concentrations selected for these studies mimic the peak plasma concentration of cisplatin (34, 35).

In conclusion, our results show that BITC targets cell viability and reduces the amount of migration and invasion of HNSCC cells, but not of normal keratinocytes. The inhibition of

migration and invasion we observed may be due to the ability of BITC to target key players involved in EMT, such as vimentin. Additionally, pretreatment with BITC chemosensitized the HNSCC cells to cisplatin by decreasing cell viability and increasing cell death suggesting that BITC could be a novel adjuvant therapy for patients with aggressive HNSCC. These initial findings warrant future *in vivo* animal studies to ensure that BITC can reach tumor cells in adequate concentrations to induce xenograft or organotypic human HNSCC tumors to undergo the changes in viability and drug sensitivity that we have documented in cell culture.

Acknowledgments

We gratefully acknowledge the Marshall University Biochemistry and Microbiology & Surgery Departments for their support. The present studies were supported by the NASA WV Space Grant Consortium, award #NNX10AK62H, and in part by NIH grants CA131395, CA140024, and WV-INBRE 5P20RR016477. The funders had no role in study design, data collection and analysis, decision to publish, or preparation of the manuscript. The content is solely the responsibility of the authors and does not necessarily represent the official views of the National Cancer Institute or the National Institute of Health. We are grateful to Dr. Johannes Fahrman for technical assistance, and Drs. W. Elaine Hardman and Richard M. Niles for critical review of the manuscript.

Abbreviations

| | |
|--------------|--|
| BITC | benzyl isothiocyanate |
| CDDP | cisplatin |
| DMSO | dimethyl sulfoxide |
| EGF | epidermal growth factor |
| EMT | epithelial mesenchymal transition |
| HNSCC | head and neck squamous cell carcinoma |
| ITC | isothiocyanate |
| MTT | 3-(4,5-dimethylthiazol-2-yl)-2,5-diphenyltetrazolium bromide |

References

1. Sayed SI, Dwivedi RC, Katna R, Garg A, Pathak KA, et al. Implications of understanding cancer stem cell (CSC) biology in head and neck squamous cell cancer. *Oral Oncol.* 2011; 47:237–43. [PubMed: 21382740]
2. de Andrade DA, Machiels JP. Treatment options for patients with recurrent or metastatic squamous cell carcinoma of the head and neck, who progress after platinum-based chemotherapy. *Current opinion in oncology.* 2012; 24:211–7. [PubMed: 22498572]
3. Kurzweg T, Mockelmann N, Laban S, Knecht R. Current treatment options for recurrent/metastatic head and neck cancer: a post-ASCO 2011 update and review of last year's literature. *European archives of oto-rhino-laryngology: official journal of the European Federation of Oto-Rhino-Laryngological Societies.* 2012; 269:2157–67.
4. Price KA, Cohen EE. Current treatment options for metastatic head and neck cancer. *Current treatment options in oncology.* 2012; 13:35–46. [PubMed: 22252884]
5. Lee DH, Kim MJ, Roh JL, Kim SB, Choi SH, et al. Distant metastases and survival prediction in head and neck squamous cell carcinoma. *Otolaryngology--head and neck surgery: official journal of American Academy of Otolaryngology-Head and Neck Surgery.* 2012; 147:870–5. [PubMed: 22581637]
6. Yoo GH, Piechocki MP, Ensley JF, Nguyen T, Oliver J, et al. Docetaxel induced gene expression patterns in head and neck squamous cell carcinoma using cDNA microarray and PowerBlot. *Clin Cancer Res.* 2002; 8:3910–21. [PubMed: 12473607]

7. Chen ZG. The cancer stem cell concept in progression of head and neck cancer. *J Oncol.* 2009; 2009:894064. [PubMed: 20052382]
8. Bourguignon LY, Earle C, Wong G, Spevak CC, Krueger K. Stem cell marker (Nanog) and Stat-3 signaling promote MicroRNA-21 expression and chemoresistance in hyaluronan/CD44-activated head and neck squamous cell carcinoma cells. *Oncogene.* 2012; 31:149–60. [PubMed: 21685938]
9. Nakamura Y. Chemoprevention by isothiocyanates: molecular basis of apoptosis induction. *Forum Nutr.* 2009; 61:170–81. [PubMed: 19367121]
10. Nakamura Y, Miyoshi N. Electrophiles in foods: the current status of isothiocyanates and their chemical biology. *Biosci Biotechnol Biochem.* 2010; 74:242–55. [PubMed: 20139631]
11. Wu X, Zhou QH, Xu K. Are isothiocyanates potential anti-cancer drugs? *Acta Pharmacol Sin.* 2009; 30:501–12. [PubMed: 19417730]
12. Cheung KL, Kong AN. Molecular targets of dietary phenethyl isothiocyanate and sulforaphane for cancer chemoprevention. *Aaps J.* 2009; 12:87–97. [PubMed: 20013083]
13. Mi L, Hood BL, Stewart NA, Xiao Z, Govind S, et al. Identification of potential protein targets of isothiocyanates by proteomics. *Chem Res Toxicol.* 2011; 24:1735–43. [PubMed: 21838287]
14. Mi L, Xiao Z, Veenstra TD, Chung FL. Proteomic identification of binding targets of isothiocyanates: A perspective on techniques. *J Proteomics.* 2011; 74:1036–44. [PubMed: 21555001]
15. Hutzen B, Willis W, Jones S, Cen L, Deangelis S, et al. Dietary agent, benzyl isothiocyanate inhibits signal transducer and activator of transcription 3 phosphorylation and collaborates with sulforaphane in the growth suppression of PANC-1 cancer cells. *Cancer Cell Int.* 2009; 9:24. [PubMed: 19712481]
16. Zhang R, Loganathan S, Humphreys I, Srivastava SK. Benzyl isothiocyanate-induced DNA damage causes G2/M cell cycle arrest and apoptosis in human pancreatic cancer cells. *J Nutr.* 2006; 136:2728–34. [PubMed: 17056792]
17. Boreddy SR, Sahu RP, Srivastava SK. Benzyl isothiocyanate suppresses pancreatic tumor angiogenesis and invasion by inhibiting HIF- α /VEGF/Rho-GTPases: pivotal role of STAT-3. *PLoS One.* 2011; 6:e25799. [PubMed: 22016776]
18. Warin R, Chambers WH, Potter DM, Singh SV. Prevention of mammary carcinogenesis in MMTV-neu mice by cruciferous vegetable constituent benzyl isothiocyanate. *Cancer Res.* 2009; 69:9473–80. [PubMed: 19934325]
19. Warin R, Xiao D, Arlotti JA, Bommarreddy A, Singh SV. Inhibition of human breast cancer xenograft growth by cruciferous vegetable constituent benzyl isothiocyanate. *Mol Carcinog.* 2010; 49:500–7. [PubMed: 20422714]
20. Amornphimoltham P, Patel V, Sodhi A, Nikitakis NG, Sauk JJ, et al. Mammalian target of rapamycin, a molecular target in squamous cell carcinomas of the head and neck. *Cancer Res.* 2005; 65:9953–61. [PubMed: 16267020]
21. Zhao L, Au JL-S, Wientjes MG. Comparison of methods for evaluating drug-drug interaction. *Frontier Bioscience.* 2010:241–9.
22. Mandal M, Myers JN, Lippman SM, Johnson FM, Williams MD, et al. Epithelial to mesenchymal transition in head and neck squamous carcinoma: association of Src activation with E-cadherin down-regulation, vimentin expression, and aggressive tumor features. *Cancer.* 2008; 112:2088–100. [PubMed: 18327819]
23. Nijkamp MM, Span PN, Hoogsteen IJ, van der Kogel AJ, Kaanders JH, et al. Expression of E-cadherin and vimentin correlates with metastasis formation in head and neck squamous cell carcinoma patients. *Radiother Oncol.* 2011; 99:344–8. [PubMed: 21684617]
24. Judson I, Kelland LR. New developments and approaches in the platinum arena. *Drugs.* 2000; 59(Suppl 4):29–36. discussion 7–8. [PubMed: 10864228]
25. Giaccone G. Clinical perspectives on platinum resistance. *Drugs.* 2000; 59(Suppl 4):9–17. discussion 37–8. [PubMed: 10864226]
26. Siddik ZH. Cisplatin: mode of cytotoxic action and molecular basis of resistance. *Oncogene.* 2003; 22:7265–79. [PubMed: 14576837]
27. Mishima M, Samimi G, Kondo A, Lin X, Howell SB. The cellular pharmacology of oxaliplatin resistance. *Eur J Cancer.* 2002; 38:1405–12. [PubMed: 12091073]

28. Keski-Santti H, Atula T, Tikka J, Hollmen J, Makitie AA, et al. Predictive value of histopathologic parameters in early squamous cell carcinoma of oral tongue. *Oral Oncol.* 2007; 43:1007–13. [PubMed: 17306608]
29. Chung FL, Jiao D, Getahun SM, Yu MC. A urinary biomarker for uptake of dietary isothiocyanates in humans. *Cancer Epidemiol Biomarkers Prev.* 1998; 7:103–8. [PubMed: 9488583]
30. Sehrawat A, Singh SV. Benzyl isothiocyanate inhibits epithelial-mesenchymal transition in cultured and xenografted human breast cancer cells. *Cancer Prev Res (Phila).* 2011; 4:1107–17. [PubMed: 21464039]
31. Steck SE, Gammon MD, Hebert JR, Wall DE, Zeisel SH. GSTM1, GSTT1, GSTP1, and GSTA1 polymorphisms and urinary isothiocyanate metabolites following broccoli consumption in humans. *J Nutr.* 2007; 137:904–9. [PubMed: 17374652]
32. Lamy E, Scholtes C, Herz C, Mersch-Sundermann V. Pharmacokinetics and pharmacodynamics of isothiocyanates. *Drug Metab Rev.* 2011; 43:387–407. [PubMed: 21554146]
33. Satelli A, Li S. Vimentin in cancer and its potential as a molecular target for cancer therapy. *Cellular and molecular life sciences: CMLS.* 2011; 68:3033–46. [PubMed: 21637948]
34. Delord JP, Puozzo C, Lefresne F, Bugat R. Combination chemotherapy of vinorelbine and cisplatin: a phase I pharmacokinetic study in patients with metastatic solid tumors. *Anticancer research.* 2009; 29:553–60. [PubMed: 19331202]
35. Ricart AD, Berlin JD, Papadopoulos KP, Syed S, Drolet DW, et al. Phase I, pharmacokinetic and biological correlative study of OSI-7904L, a novel liposomal thymidylate synthase inhibitor, and cisplatin in patients with solid tumors. *Clin Cancer Res.* 2008; 14:7947–55. [PubMed: 19047127]

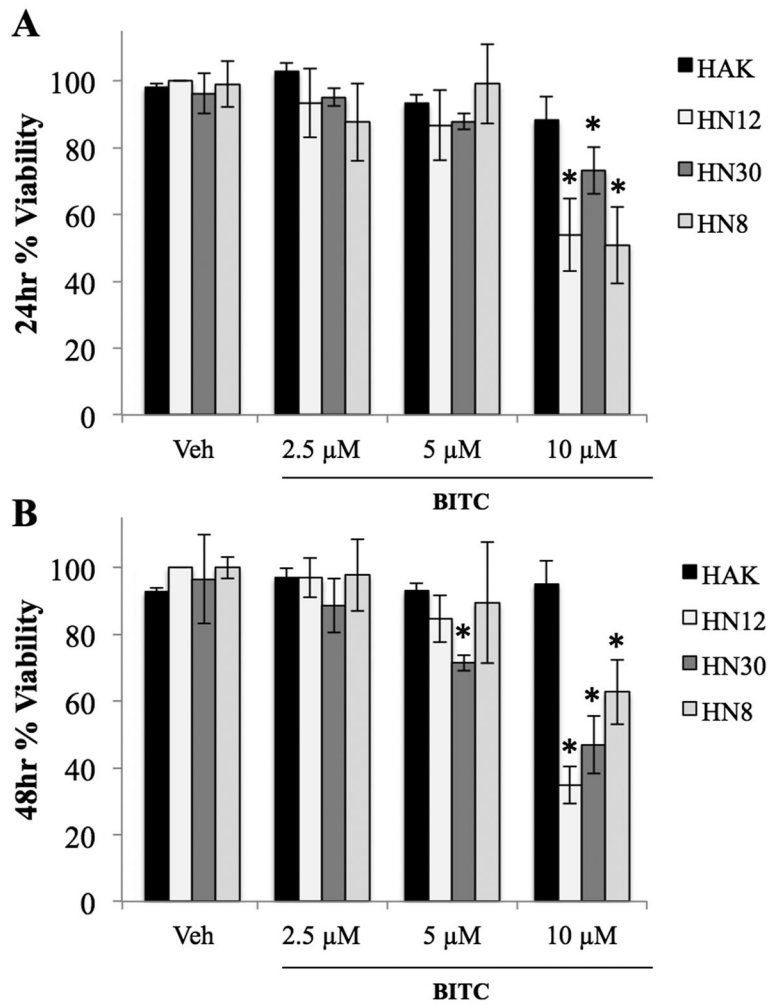


FIG. 1. HNSCC percent viability measured by MTT assay following exposure to BITC treatments compared to negative controls. (A) Percent viability of HAK, HN12, HN30 and HN8 cells at 24 hours. (B) Percent viability of HAK, HN12, HN30 and HN8 cells at 48 hours. (*) indicates significant difference from respective cell line vehicle control. Error bars represent standard deviation. One-way ANOVA for multiple comparisons with Dunnet's Post-Hoc test (* $p < 0.05$).

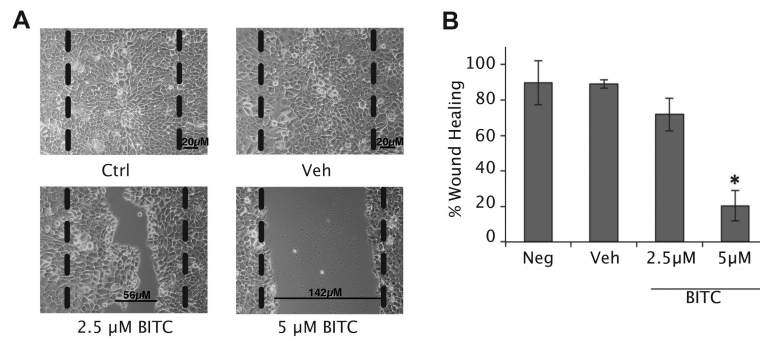
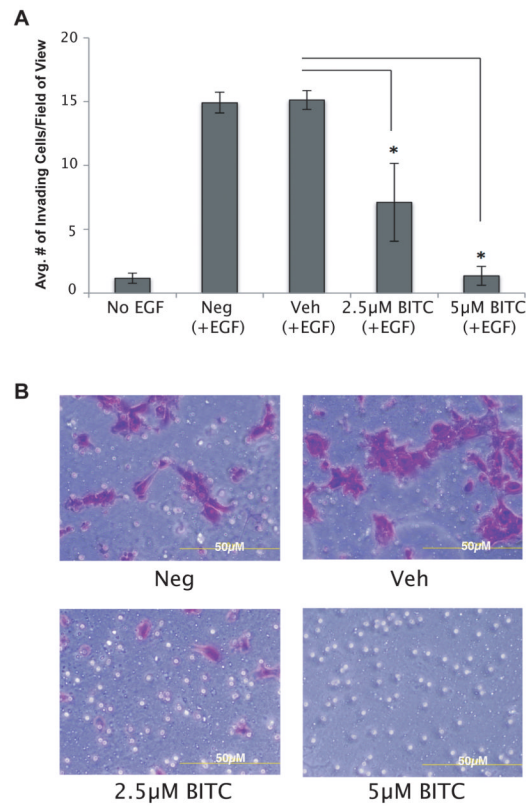


FIG. 2. BITC inhibited wound-healing of HN12 cells after 24 hours. (A) Inverted light microscope pictures of HN12 cells before and after BITC treatment (2.5–5µM). Dashed lines represent scratch size before treatment. Vehicle control was DMSO. Magnification 100X. (B) Bar diagram represents the percent wound healing determined after 24 hours using wound size measurements. Error bars represent standard deviation. One-way ANOVA for multiple comparisons with Dunnet's Post-Hoc test (* $p < 0.05$).

**FIG. 3.**

Invasion assay of HN12 cells following BITC treatment at 24 hours. (A) Bar diagram represents the average number of invading cells/field of view counted at 24 hours following a 1-hour treatment of HN12 cells with BITC. EGF was used as chemoattractant. Error bars represent standard deviation. One-way ANOVA for multiple comparisons with Dunnet's Post-Hoc test ($*p < 0.05$). (B) Inverted light microscope pictures of HN12 cells stained with crystal violet following BITC treatment. NEG: negative control. VEH: vehicle control. Magnification x200.

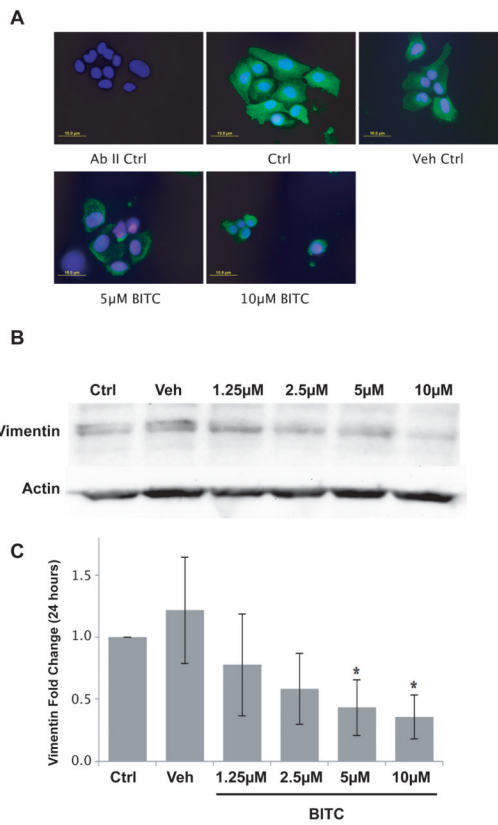


FIG. 4. Vimentin expression in HN12 cells following one-hour treatment with a range of concentrations of BITC. (A) Representative immunofluorescence images of a vimentin immunostaining acquired with an inverted epifluorescence microscope before and after 1-hour treatment of HN12 cells with a range of concentrations of BITC (5–10µM). Anti-vimentin (1:400); AbII anti-rabbit Alexa Fluor 488 (1:200); DAPI to counterstain the nuclei. Magnification 400X. Bar size is 10µm. (B) Western blot analysis of vimentin expression in HN12 cells after 1-hour treatment with a range of concentrations of BITC (1.25–10µM). Actin was used to normalize the blot. (C) Densitometric analysis of vimentin and actin protein expression. Diagram represents the fold change of vimentin after 24 hours normalized to actin control. One-way ANOVA for multiple comparisons with Dunnett’s Post-Hoc test (**p* 0.05).

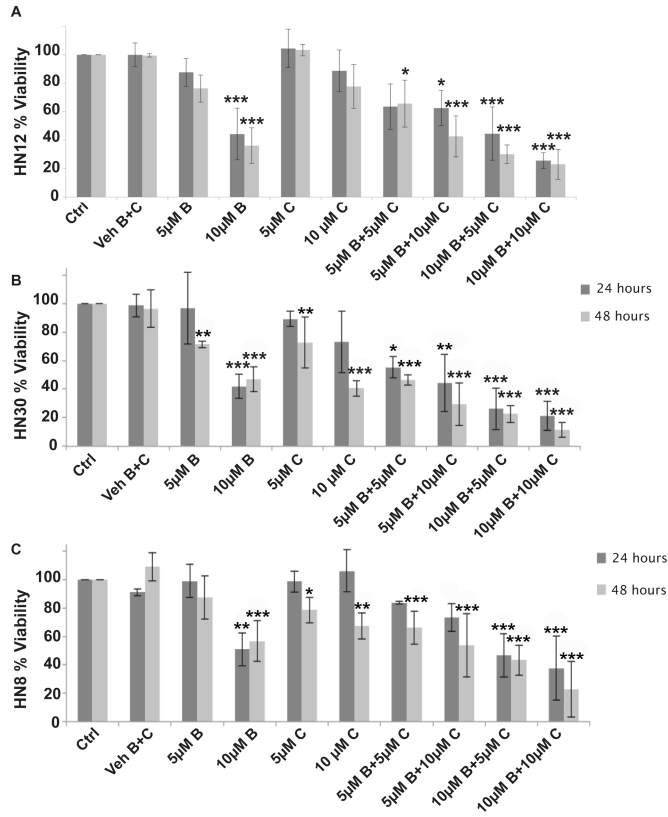


FIG. 5. MTT viability assay of HNSCC cells following treatment with BITC, CDDP, or a combination of BITC followed by CDDP compared to controls. (A) Diagram represents the percent of HN12 viable cells after 24 and 48 hours following BITC, CDDP, or a pretreatment of BITC followed by a CDDP treatment (24 hours CI= 0.86; 48 hours CI= 0.93). (B) Diagram represents the percent of HN30 viable cells after 24 and 48 hours following BITC, CDDP, or a pretreatment of BITC followed by a CDDP treatment (24 hours CI= 0.79; 48 hours CI= 0.52). (C) Diagram represents the percent of HN8 viable cells after 24 and 48 hours following BITC, CDDP, or a pretreatment of BITC followed by a CDDP treatment (24 hours CI= 1.09; 48 hours CI= 0.73). Dark grey bars indicate cell viability at 24 hours; light grey bars indicate cell viability at 48 hours. Error bars represent standard deviation. One-way ANOVA for multiple comparisons with Dunnet’s Post-Hoc test (**p* 0.05; ***p* 0.001; ****p* 0.0001).

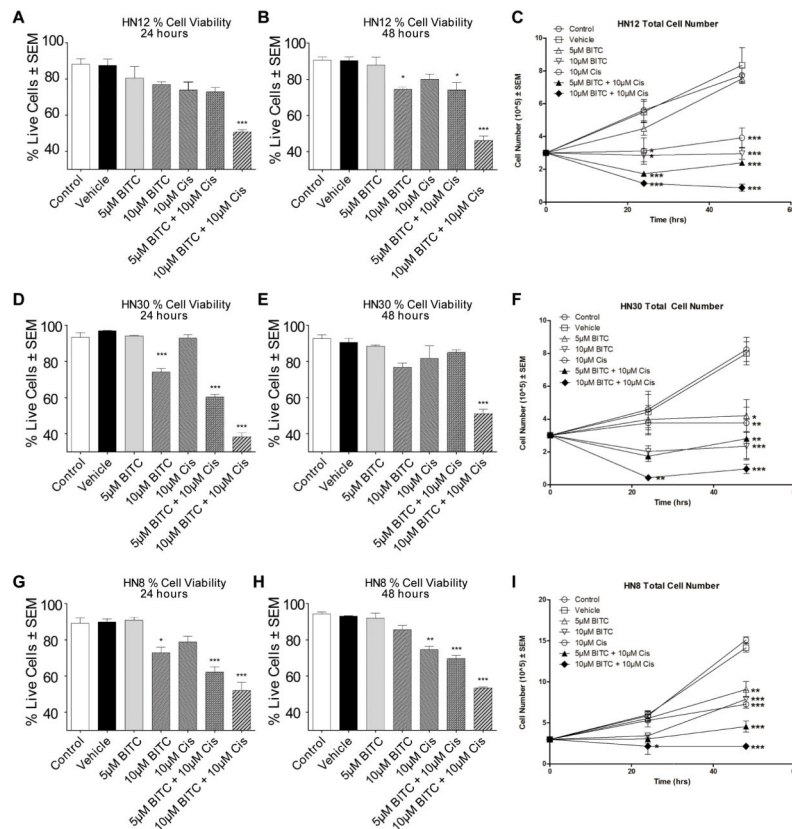


FIG. 6. Dead/Live cell viability assay and cell counts of HNSCC cells following treatment with BITC, CDDP, or a combination of BITC followed by CDDP. (A–B) Diagrams represents the percent of HN12 live cells after 24 (A) and 48 (B) hours following BITC, CDDP, or a pretreatment of BITC followed by a CDDP treatment. (C) Diagram shows the total cell number of HN12 cells after 24 and 48 hours following BITC, CDDP, or a pretreatment of BITC followed by a CDDP treatment. (D–E) Diagrams represents the percent of HN30 live cells after 24 (D) and 48 (E) hours following BITC, CDDP, or pretreatment of BITC followed by a CDDP treatment. (F) Diagram shows the total cell number of HN30 cells after 24 and 48 hours following BITC, CDDP, or a pretreatment of BITC followed by a CDDP treatment. (G–H) Diagrams represents the percent of HN8 live cells after 24 (G) and 48 (H) hours following BITC, CDDP, or a pretreatment of BITC followed by a CDDP treatment. (I) Diagram shows the total cell number of HN8 cells after 24 and 48 hours following BITC, CDDP, or a pretreatment of BITC followed by a CDDP treatment. Error bars represent standard error. One-way ANOVA for multiple comparisons with Dunnet’s Post-Hoc test (**p* 0.05; ***p* 0.001; ****p* 0.0001).

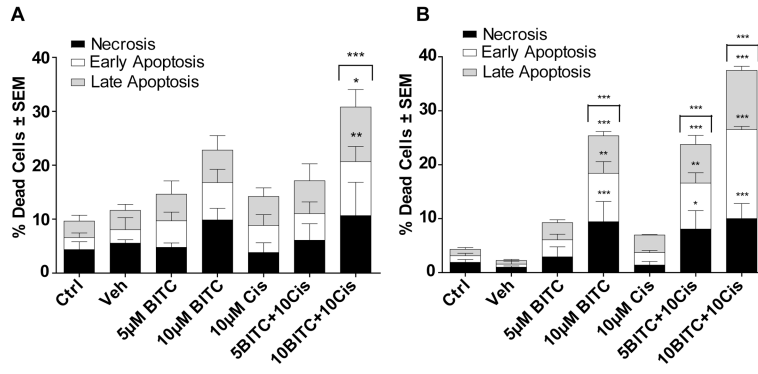


FIG. 7. Annexin-V assay of HN12 and HN30 cells following treatment with BITC, CDDP, or a combination of BITC followed by CDDP. (A) Diagram represents the percent of HN12 dead cells after 24 hours following BITC, CDDP, or a pretreatment of BITC followed by a CDDP treatment. (B) Diagram represents the percent of HN30 dead cells after 24 hours following BITC, CDDP, or a pretreatment of BITC followed by a CDDP treatment. Black bars represent necrosis, white bars early apoptosis, grey bars late apoptosis. Error bars represent standard error. One-way ANOVA for multiple comparisons with Dunnet’s Post-Hoc test (**p* 0.05; ***p* 0.001; ****p* 0.0001).